

## 2.1 Magnets

2.1.1	Magnet System General Description	1
2.1.1.1	System Description and Main Parameters	1
2.1.1.2	Physical and Functional Interfaces	4
2.1.1.3	Heat Loads	6
2.1.2	Magnet Structures	7
2.1.2.1	Description	7
2.1.2.2	TF Magnet Structural Assessment	14
2.1.3	Conductor Design	18
2.1.3.1	Conductor Design Criteria	18
2.1.3.2	TF Conductor	19
2.1.3.3	CS Conductor	21
2.1.3.4	PF Conductor	22
2.1.3.5	CC Conductor	24
2.1.4	TF Coils Manufacture	24
2.1.4.1	TF Coil Winding Pack	25
2.1.4.2	TF Coil Cases	26
2.1.5	Central Solenoid Manufacture	27
2.1.5.1	Flux Generation and Conductor Jacket Options	27
2.1.5.2	CS Winding Pack	28
2.1.5.3	CS Preload Structure	29
2.1.5.4	CS Joints and Helium Pipe Inlets	30
2.1.5.5	CS Structural Assessment	31
2.1.6	PF Coils Manufacture	32
2.1.6.1	PF Winding Packs	32
2.1.6.2	PF Joints and Helium Pipe Inlets	33
2.1.7	Correction Coils Manufacture	33
2.1.8	Auxiliary Systems	34
2.1.8.1	In-cryostat Feeders	34
2.1.8.2	Cryostat Feedthrough	36
2.1.8.3	Coil Terminal Box and Structure Cooling Valve Boxes	36
2.1.8.4	Instrumentation	37
2.1.9	Magnet Safety	38
2.1.10	Supporting R&D and General Assessment	38

### 2.1.1 Magnet System General Description

#### 2.1.1.1 System Description and Main Parameters

The magnet system for ITER consists of 18 toroidal field (TF) coils, a central solenoid (CS), six poloidal field (PF) coils and 18 correction coils (CCs). The magnet system elevation is shown on Figure 2.1.1-1.

The TF coil cases, which enclose the TF coil winding packs, form the main structural component of the magnet system. The TF coil inboard legs are wedged all along their side walls in operation, with friction playing an important role in supporting the out-of-plane magnetic forces. In the curved regions above and below the inboard leg, the out-of-plane loads are supported by four upper and four lower poloidal shear keys arranged normal to the coil centreline. In these regions, the coils are linked by means of two upper and two lower pre-compression rings which provide a radial centripetal force and improve the operation of the shear keys. In the outboard region, the out-of-plane support is provided by four sets of outer intercoil structures (OISs) integrated with the TF coil cases and positioned around the perimeter within the constraints provided by the access ducts to the vacuum vessel. The

OISs are structures acting as shear panels in combination with the TF coil cases. There is low voltage electrical insulation between TF coils in the inboard leg wedged region and between the OIS connecting elements in order to avoid the circulation of eddy currents.

N 10 GR 1 00-12-07 W 0.1

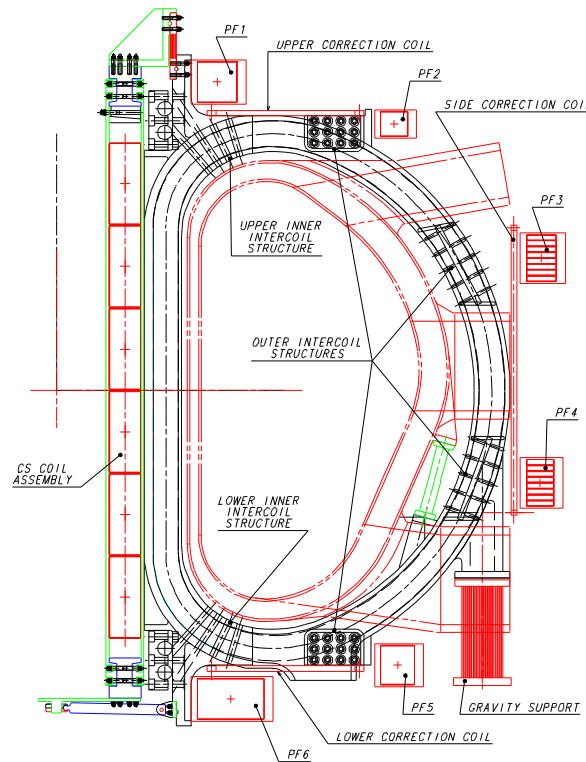


**Figure 2.1.1-1 Magnet System Elevation**

The CS consists of a vertical stack of six independent winding pack modules. The stack is hung from the top of the TF coils through flexible supports and is provided at the bottom with a locating mechanism which acts as a support against dynamic horizontal forces. The CS pre-load structure, which consists of a set of tie-plates located outside and inside the coil stack, provides axial pressure on the stack. The number of CS modules has been selected to satisfy the plasma equilibrium requirements. The CS coil stack is self-supporting against the coil radial forces and most of the vertical forces, with the support to the TF coils reacting only the weight and net vertical components resulting from up-down asymmetry of the poloidal field configuration.

The six PF coils (PF1 to PF6) are attached to the TF coil cases through supports which include flexible plates or sliding interfaces allowing radial displacements. The PF coils provide suitable magnetic fields for the plasma equilibrium and control and their position and size have been optimized accordingly, within the constraints imposed by the access to the in-vessel components.

Outside the PF coils are located three independent sets of correction coils (CCs), each consisting of six coils arranged around the toroidal circumference above, at and below the equator. These coils are used to correct non-axisymmetrical error fields arising from errors in

the position of the TF coils, CS and PF coils and from the NB injection magnetic field correction system, and to stabilise plasma resistive wall modes.

Both CS and TF coils operate at high field and use Nb<sub>3</sub>Sn-type superconductor. The PF coils and CCs use NbTi superconductor. All coils are cooled with supercritical helium in the range 4.4 - 4.7K. The conductor type for the TF coils, CS and PF coils is a circular cable-in-conduit multistage cable with about 1,000 strands cabled around a small central cooling spiral tube. The operating currents are 40 - 46 kA for the CS and PF coils and 68 kA for the TF coils. The CCs use a reduced size conductor (about 300 strands) without the central cooling channel.

The coil turn and ground electrical insulation consists typically of multiple layers of kapton-glass impregnated with epoxy resin. Epoxy-glass is used extensively to fill tolerance gaps. The CS and PF coils are pancake wound with a conductor that has a square outer section. The TF coils use a conductor with a circular outer section that is contained in grooves in so-called "radial plates". There is one radial plate for each double pancake and the conductor is contained in grooves on each side.

Gravity supports, composed of pedestals and flexible elements (one under each TF coil), support the whole magnet system. Each TF coil is electrically insulated from its own support to avoid the circulation of eddy currents between TF coils. The TF coil case also supports the vacuum vessel (VV) and in-vessel component weight and operational loads.

All TF coils, the CS and the upper and outer PF coils (PF1 to PF4) are designed to be removable from the machine in case of a major fault. Individual double pancakes of the PF coils may be disconnected and by-passed in situ in case of fault, since the PF coils have accessible joints located on their external side. In addition, the cryostat design allows the lower (trapped) PF coils (PF5 and PF6) to be rewound in situ under the machine.

In Tables 2.1.1-1, 2 and 3 the main magnet parameters are listed.

**Table 2.1.1-1 Overall Magnet System Parameters**

Number of TF coils	18
Magnetic energy in TF coils (GJ)	~ 41
Maximum field in TF coils (T)	11.8
Centring force per TF coil (MN)	403
Vertical force per half TF coil (MN)	205
TF electrical discharge time constant (s)	11
CS peak field (T)	13.5
Total weight of magnet system (t)	10,130

**Table 2.1.1-2 Parameters for TF Coils and CS**

	TF Coil	CS *
		Modules CS 1, 2, 3
Overall weight (including structures) (t)	312x18	925
Coil current (MA)	9.13	24.2 at EOB (12.8 T)
Number of turns per TF coil / CS module:		
Radial	11	14
Toroidal / Vertical	14	38
Total	134	522
Conductor unit length (m)	760 (double pancakes)	881 (for 6 pancakes) 579 (for 4 pancakes)
Turn voltage (V)	26.5 (discharge)	20 (IM)
Ground/Terminal voltage (kV) in normal operation	3.55 / 3.55 ** (2 coils in series)	5 / 10
Number of current lead pairs	9	6 ***

\* CS parameters are for the design option using an Incoloy square jacket

\*\* A voltage surge (of a few ms) caused by the jitter of the switches may reach about 5 kV.

\*\*\* The current leads for CS modules 1 (upper and lower) are connected in series outside the machine and the power supplies and discharge units are interleaved to limit the ground voltage to 5 kV in normal operation.

**Table 2.1.1-3 Parameters for PF Coils**

	PF1	PF2	PF3	PF4	PF5	PF6
Winding weight (t)	145	129	385	353	255	263
Max. coil current capacity (MA)	11.34	4.39	8.46	7.74	9.90	19.26
Number of turns per coil:						
Radial	16	11	12	11	14	27
Vertical	16	10	16	16	16	16
Total	252	107	118	172	220	428
Conductor unit length (m) (double pancake, two-in-hand)	392	560	884	807	727	723
Maximum Turn voltage (V)*	625	1750	875	1000	875	714
Ground/Terminal voltage (kV)*	5/10	7/14	7/14	7/14	7/14	5/10

\* Turn voltages are for a two-in hand winding configuration. For PF2 to PF5, a vertical stabilisation voltage of 9 kV (on-load voltage) is assumed, allowing 3 kV above the present 6 kV converter design for possible upgrades.

### 2.1.1.2 Physical and Functional Interfaces

The magnets are located within the cryostat which provides the thermal insulation for the 4.5K superconducting coils from the ambient heat load. This is done by a vacuum within the cryostat to eliminate the convective heat loads, and by the use of intermediate thermal shields at 80K to intercept the bulk of the thermal radiation and conduction from the cryostat and the vacuum vessel.

Feeders to the coils include the superconducting busbars, cryogen service lines, and instrumentation cables. These feeders run from individual coil terminals inside the cryostat, through cryostat feedthroughs (CF) and into coil terminal boxes (CTBs) or structure cooling valve boxes (SCVBs). These boxes are located outside the cryostat and bioshield, in the tokamak galleries which are accessible for hands-on maintenance. The interfaces between the magnet system and the power supplies and the cryoplant are at these boxes.

### *Power Supplies*

The interface between power supplies and the magnets occurs at the CTBs where the transition is made from superconducting busbars to room temperature (water-cooled aluminium) busbars.

The power supplies have two physical interfaces to the magnets.

- i) The current supplies and discharge circuits for the coils. These consist of one supply for the 18 TF coils plus 9 discharge resistors connected between each coil pair. Each PF and CS coil module has its own supply and discharge resistor.
- ii) The magnet structure grounding scheme. The magnet structures are all connected to ground through the busbar containment pipes to the cryostat wall. The connection of the cryostat into the overall machine grounding scheme is part of the power supplies.

### *Cryoplant*

The boundary between the cryoplant system and the magnet helium manifolding occurs at the CTBs and SCVBs. These boxes contain the adjustable valves that allow the proper distribution of the helium flow into the magnet components.

In operation, the cryoplant provides supercritical helium to the four sets of coils (TF, CS, PF and CCs), their superconducting busbars, and the magnet structures. The coils, busbars and structure cooling systems are subdivided into a number of closed loops where supercritical helium is circulated by a pump and recooled through a primary heat exchanger located in the auxiliary cold boxes of the cryoplant. For the coils, the supercritical helium is supplied in the temperature range of 4.4 - 4.7K. The cryoplant also supplies liquid helium to the current leads and receives back gaseous helium at room temperature from these current leads.

For the cooldown of the magnet system, the primary heat exchanger is bypassed and cold gaseous helium is passed directly from the cryoplant compressors through the magnets and structures. In this phase, the maximum temperature difference between coil/structure inlet and outlet flows is 50K to limit thermal stresses, and the cooldown rate is about 0.5K/hr. Once the magnet temperature reaches 80K, helium at about 5K can be supplied by the cryoplant and gaseous helium returned from the coils. Once the coils reach the operating temperature, the pump and primary heat exchanger are put back into the circuit.

In the case of a TF coil quench (including the TF coil quench which occurs after a fast discharge), the primary circuit is vented initially to a cold holding tank at 80K and then to tanks at 300K if the capacity of the cold storage is exceeded. The vent opening pressure in the primary loop is 1.8 MPa.

### 2.1.1.3 Heat Loads

During operation, heat from external sources and from the magnets themselves is deposited in the magnet system. Thermal radiation from the 80K cryostat thermal shield is deposited on the outer surface of the TF coil cases and structures and the PF coils. Thermal radiation from the vacuum vessel shield is deposited on the TF coil case inner surfaces. Heat is conducted from the machine gravity supports, the vacuum vessel supports and the vacuum vessel thermal shield supports.

Nuclear heat is the dominant heat load for the TF coils and is essentially deposited along the inner surface of the inboard legs. Table 2.1.1-4 shows the distribution of the nuclear heat in the TF coil cases and winding pack. The values shown are used for the assessment of the coil performance and may not reflect the latest details of shielding design. Nuclear heat is also deposited in the PF coils in the vicinity of the vessel ports. There is also heat from gamma radiation due to the activation ( $^{16}\text{N}$ ) of the cooling water of in-vessel components. This heat load is small and is deposited essentially in PF coils and feeders in the vicinity of the heat transfer system pipes. All external heat loads are summarized in Table 2.1.1-5, which also shows the internal heat loads due to the operation of the magnets. These include AC losses in conductors, eddy current losses in structures, and resistive losses in joints. The table also includes the losses associated with the magnet feeders and the liquid helium requirements to cool the current leads where the transition is made from superconducting busbars to room temperature busbars.

**Table 2.1.1-4 Nuclear Heating in the TF Coils (kW)  
for the 15 MA Reference Scenario with a Total Fusion Power of 500 MW**

	<b>Inboard Leg</b>	<b>Behind Divertor</b>	$^{16}\text{N}$	<b>Around Ports</b>	<b>Total</b>
Coil Case	4.82	1.50	0.4	1.56	8.28
Winding Pack	5.11	0.31			5.42
<b>Total</b>	<b>9.93</b>	<b>1.81</b>	<b>0.4</b>	<b>1.56</b>	<b>13.70</b>

**Table 2.1.1-5 Heat Loads in the Magnets and Liquid Helium Requirements for Current Leads (15 MA Reference Scenario with a Total Fusion Power of 500 MW)**

Heat loads	TF cases & structures	TF winding	PF & corr. coils	CS & CS structure	Total**
Nuclear heating	8.28 kW during burn	5.42 kW during burn	0.40 kW during burn	0	Average value 3.13 kW
AC & eddy current losses	5.50 MJ	1.36 MJ*	0.78 MJ*	5.28 MJ*	Average value 7.17 kW
Joints	0.0	1.00 kW	0.08 kW average	0.05 kW average	1.13 kW average
Thermal radiation Cryostat Vacuum vessel	5.20 kW 0.28 kW	0	0.11 kW	0.01	5.60 kW
Thermal conduction Gravity supports VV supports Thermal shield	2.0 kW 1.7 kW 0.1 kW	0	0	0	3.8 kW
He feeders, SC bus bars and CTBs	0.77 kW		0.66 kW	0.37 kW	1.8 kW
Helium flow rates for current leads	0.0	61.2 g/s	19.1 g/s	16.1 g/s	96.4 g/s

\* A coupling loss time constant of 50 ms is assumed.

\*\* The average values are for a 400 s burn with a 1800 s pulse repetition.

## 2.1.2 Magnet Structures

### 2.1.2.1 Description

The TF magnet is subjected to two main force systems. The in-plane loads are generated by the interaction of the current in the TF coils with the toroidal field. The out-of-plane loads are generated by the interaction of the current in the TF coils with the poloidal field. The TF coil cases are the main structural component of the magnet system and they provide support against the TF coil in-plane as well as out-of-plane loads. The PF coils, CS and vacuum vessel are attached to the TF coil cases through supports which are rigid in the vertical and toroidal directions but flexible in the radial direction. In this way, the TF coil cases connect all the PF coils and the CS with the vacuum vessel, and balance all the electromagnetic forces within the magnet assembly. This arrangement results in a compact design without load transmission to structures external to the TF coil cases. Figure 2.1.2-1 shows a TF coil case with all attachments.

N 11 GR 645 01-05-30 W 0.1

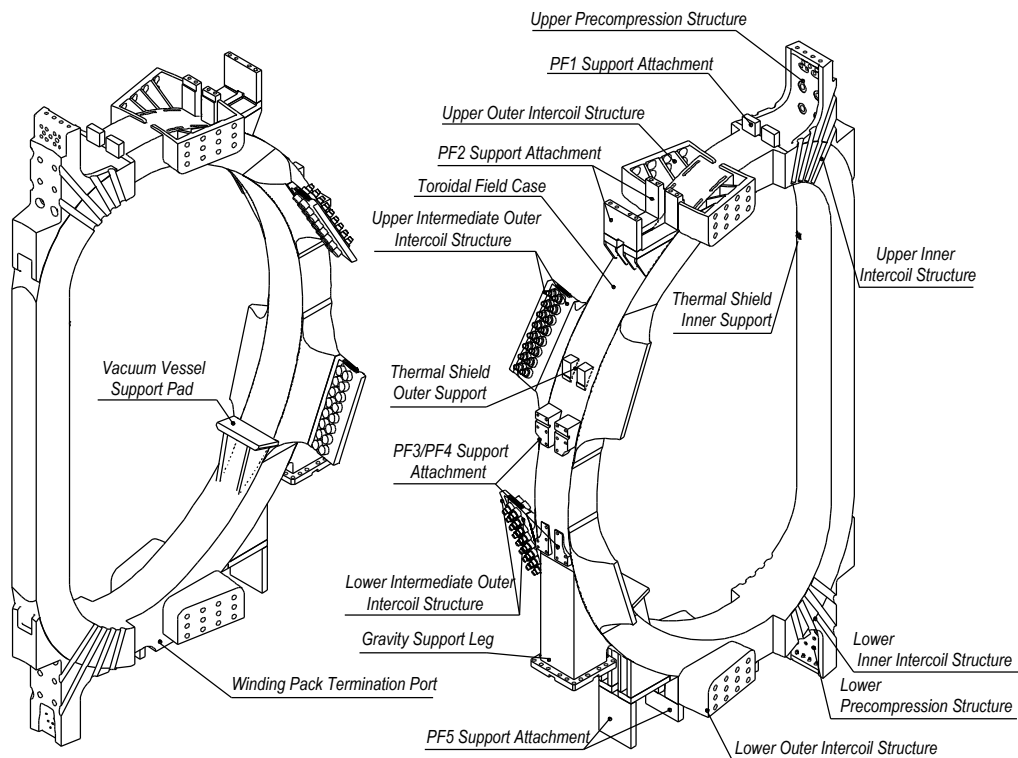


**Figure 2.1.2-1 TF Coil Case**

### *Inboard Region*

The centring force on each TF coil is reacted by toroidal hoop pressure in the central vault formed by the straight inboard legs of the coils. The front part or “nose” of each coil case is thickened for this purpose. All along their inboard legs, the coil cases are wedged over their full radial thickness. About 40% of the centring force is reacted through the winding pack of the coil and 60% is reacted by the case. The wedging surfaces must be accurately matched to achieve the required magnetic alignment and reduce stress peaks under the large toroidal wedging pressure of about 590 MPa at the “nose” of the coil cases. Machining of the wedging surfaces will ensure that deviations from flatness have only long wavelength and do not result in localised peak stress. Systematic errors, in particular on the wedge angle, could result in significant stress intensification and must be kept within tolerable limits. Analysis has shown that a local assembly gap of 0.4 to 0.6 mm between adjacent wedging surfaces is acceptable, even if all coils have the same error. For each coil, the flatness tolerance band is therefore 0.2 to 0.3 mm and this is considered achievable by precision machining.

Insulation is required between coils to avoid eddy current flow from coil to coil. The insulation will consist of a thin layer of epoxy-glass or ceramic coating which must resist the essentially static compressive load of 590 MPa. R&D activities have been initiated to cover this requirement. A high friction factor is required as friction transmits a significant fraction of the overturning moments. The minimum acceptable friction factor is about 0.2 and it is desirable to achieve higher values.

### Inner Intercoil Structures

The inner intercoil structures (IISs) are situated at the inboard curved regions, immediately above and below the inboard straight leg of the TF coils (Figure 2.1.2-2). These regions are particularly critical because this is where the out-of-plane loads are highest and the space available for structures is restricted between the TF coils. At each IIS, the cyclic out-of-plane loads are resisted by a set of four shear keys between the coils. The keys run normal to the coil centreline in key slots machined in the coil case, which is locally thickened. The keys prevent the development of torsion in the cases, which can make a large contribution to the case tensile stresses. At the same time, the relative flexibility of the case in bending gives an almost uniform poloidal distribution of load on the four keys. The shear load per key is in the range of 15 to 19 MN.

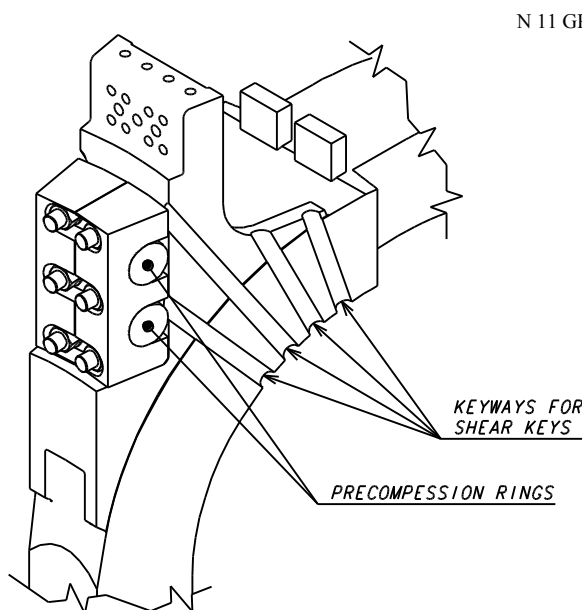


**Figure 2.1.2-2 Inner Intercoil Structure**

In the inboard curved region, the radial expansion of the coils during energisation results in the opening of toroidal gaps between adjacent cases. Although small, the radial movement is sufficient to create a toroidal gap of about 0.35 mm between key and key slot. During plasma operation, the shear loads acting on the keys tend to increase this gap to more than 1 mm. In order to suppress this undesirable effect, and ensure that the keys do not become loose in their slots, the TF coils are put under a centripetal pre-load at assembly. This pre-load is provided by two pre-compression rings at the top and bottom of the TF coil inboard legs. The rings are tensioned at assembly and the load is transmitted to the TF coils by bolts oriented in the radial direction. The TF coils are therefore put into toroidal compression. Analysis shows that with a radial centripetal pre-load of 60 - 70 MN per TF coil, the toroidal separation in the key region is almost completely eliminated. To be effective, these pre-compression rings need to have a significantly lower elastic modulus than that of the case, so that the pre-compression is not sensitive to assembly tolerances. In view of the limited space available, the rings require a high strength material. Finally, the rings should have a high electrical resistance to avoid the circulation of excessive eddy currents. A material satisfying these requirements is a unidirectional glass fibre-epoxy composite which can be made using a wet glass fibre (S-glass) filament winding technique. The stresses in the rings are limited by pre-tensioning at room temperature since the material is stronger at 4K. There are no significant

extra stresses due to the out-of-plane movements of the TF coils. Table 2.1.2-1 summarises the main requirements for the rings. R&D activities to establish the allowable stress and creep behaviour of unidirectional glass fibre composites are under discussion.

**Table 2.1.2-1 Mechanical Parameters for Pre-compression Rings**

<b>Material</b>	<b>Peak tensile stress at room temperature (MPa)</b>	<b>Cross-sectional area of two rings (m<sup>2</sup>)</b>	<b>Radial displacement to apply pre-compression (mm)</b>
Fibreglass	587	0.22	~ 23

The pre-compression rings increase the overall stiffness of the IIS and contribute to lowering stresses in this region, thus increasing the fatigue life of the TF coil case.

### ***Outer Intercoil Structures***

There are four OISs. The upper and lower OISs are located respectively above the upper ports and below the divertor ports of the vacuum vessel. The upper and lower intermediate OISs are located respectively above and below the equatorial ports.

The OISs directly above and below the equator are required to support the out-of-plane forces on the outboard part of the coil. There is a large shear force (in the vertical direction) of about 20 MN acting on each of these two OISs. There is also a toroidal tensile load due to the radial expansion of the coil outboard leg. The pre-load provided by the pre-compression rings significantly reduces this toroidal tension to values of about 8 MN per OIS.

The poloidal extent of the two equatorial OISs belts is limited by the vertical size of the vacuum vessel ports and, due to this limitation, relatively high cyclic stresses occur at the re-entrant corners where the OISs connect to the TF coil cases. Local structural reinforcements and smooth transitions are required to keep stresses within allowable limits. In the current design, the OISs consist of shear panels, with a thickness of about 130 mm, protruding from the side walls of the case. Shear load transmission is provided by multiple-finger friction joints which are welded to the two adjacent shear panels after survey at assembly. The joints are pre-loaded by two rows of insulated bolts acting on the fingers separated by insulated washers. With this multiple-finger arrangement, the friction surfaces and the shear capability of each bolt is multiplied by 5. The cross section of a friction joint is shown in Figure 2.1.2-3. Access to the vacuum vessel supports is required during the tokamak assembly and is available before welding of the multi finger joint.

N 11 GR 557 00-12-07 W 0.1

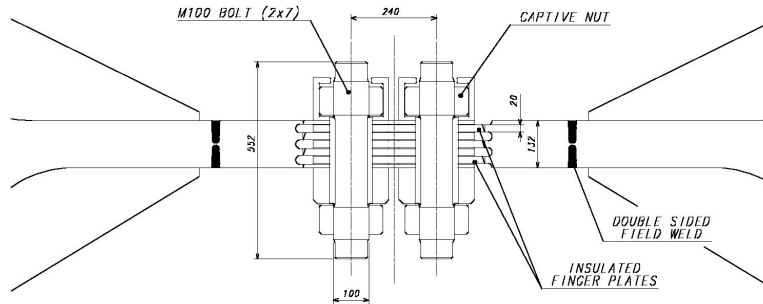


**Figure 2.1.2-3 Cross Section of Friction Joint**

As an alternative to this friction joint design, a box structure integral to the case has been developed (Figure 2.1.2-4). In this design, shear load transmission is accomplished by insulated bolts and shear keys. This box structure includes a removable central part which is required to gain access to the vacuum vessel supports during assembly. The box structure has been analysed and found to provide adequate out-of-plane support. Its advantage, as compared to the friction joint, is to eliminate in-situ welding. It requires, however, precision machining of the keyways. The final choice between these 2 design options will be made taking manufacturing aspects and cost into consideration.

N 11 GR 647 01-05-30 W 0.1

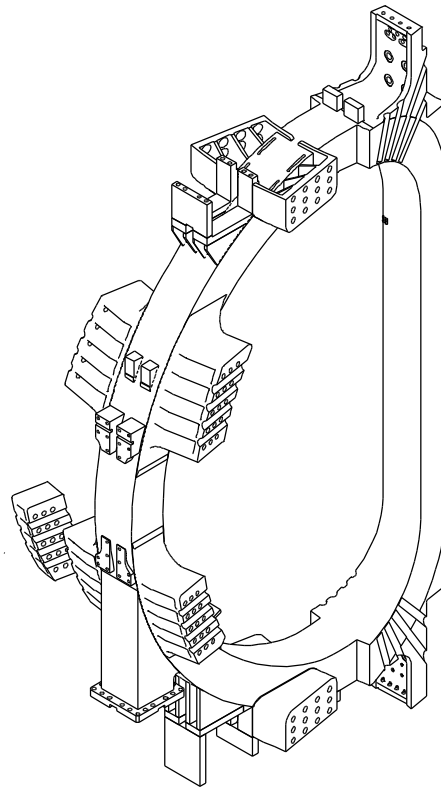


**Figure 2.1.2-4 Coil Case showing the Alternative OIS Box Design**

### *Vacuum Vessel Supports*

The vacuum vessel supports are attached to the TF coils at a poloidal location just below the equatorial port level, thus minimizing the distance from the TF coil gravity support pedestals. This reduces the toroidal rotation of the whole vessel during machine pulses. These supports are of laminated construction to allow differential radial displacements between the TF coils and the vacuum vessel while providing toroidal registration. The supports are designed to resist gravity, seismic and all electromagnetic loads on the vacuum vessel. The supports must also transmit bending moments caused by vacuum vessel deformations and by TF coil tilting motions.

The thermal load from the hot vessel to the TF coil cases is reduced by a thermal “anchor” consisting of cooling channels for 80K helium gas, half way up the support.

### *Gravity Supports*

The gravity supports for the machine are shown on Figure 2.1.2-5. They are placed under the outer curved region of each TF coil between the PF4 and PF5 coils. Electrical insulation is placed between each TF coil and the top surface of the support pedestal to avoid eddy currents. The machine gravity support pedestals are equipped with flexible plates, so that they can deflect in the radial direction to allow thermal contraction or expansion of the magnet system, but they are rigid against out-of-plane bending caused by TF coil out-of-plane displacement or seismic motion. The pedestals are connected, at their lower ends, to a rigid supporting ring, which is an integral part of the cryostat structure. This ring resists the bending moments transmitted by the pedestals but transfers horizontal seismic loads to the building through horizontal tie plates. The gravity load is transferred to the building through 18 cylindrical support columns (Figure 2.1.2-5).

N 11 GR 559 00-12-07 W 0.1

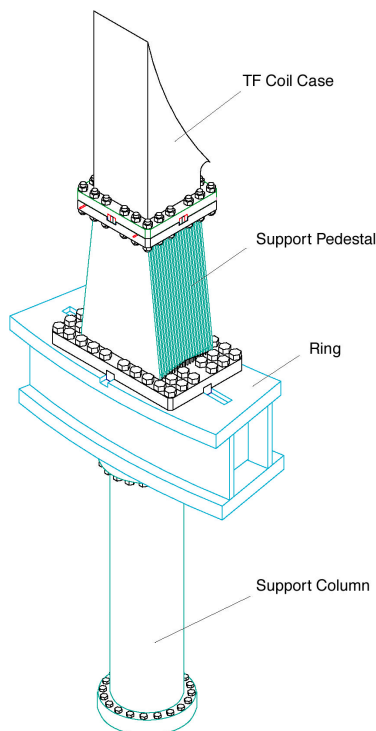


**Figure 2.1.2-5 Gravity Support**

Thermal conduction from the room temperature supporting ring to the TF coils is reduced by a thermal anchor consisting of cooling channels for 80K helium gas, at a distance of about 600 mm below the top flange of the support pedestals.

Analysis of the gravity supports has been carried out under a number of load combinations which include gravity loads, seismic loads and imposed displacements or moments associated with the motion of the magnets due to thermal contraction and electromagnetic loads. The design meets all requirements for both room and operating temperature conditions.

### *PF Coil Supports*

Each of the PF coils is self-supporting with regard to the radial magnetic loads, and the supports for these coils have been designed to allow for free radial expansion of the coils by using flexible plates or sliding supports. The vertical and lateral loads on each PF coil are transmitted through these supports to the TF coil cases. There are also bending moments due to the tilting motion of the TF coils which is transmitted from the TF coils to the PF coils.

The PF2 to PF5 coils have 18 supports while, because of their smaller diameter, the PF1 and PF6 coils have only 9 supports around their toroidal circumference. A typical support is shown on Figure 2.1.2-6. At each PF coil support, the winding pack is clamped between a pair of plates linked by tie-rods. For the PF2 to PF5 coils, there are flexible plates which provide the link between the TF coil case and one of the clamping plates. For the PF1 and PF6 coils, sliding supports have been provided due to space limitations. For these sliding supports, a low friction material (fibreslip) is placed directly between the clamping plates and the TF coil case surfaces.

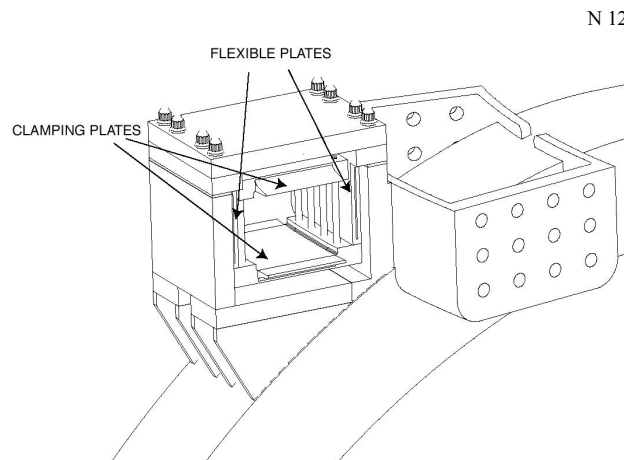


**Figure 2.1.2-6 PF2 Coil Clamp (winding pack not shown)**

### 2.1.2.2 TF Magnet Structural Assessment

#### *Structural Design Criteria*

The stresses are assessed in terms of plasticity (static limit), fast fracture and fatigue behaviour.

The static stress limit is dependent on the material and the static stress system it has to support. Following the ITER structural design criteria for materials at cryogenic temperatures, operation up to 2/3 of the yield stress is allowed for primary membrane stress systems and up to 30% above this for primary membrane plus bending stresses. For welds, these values are decreased by factors specified in the design criteria. The material is assumed to be one of the family of strengthened austenitic steels defined in ITER materials specifications that have been developed for cryogenic applications.

The fatigue assessment method, which is applied to the TF coil cases, uses a crack growth analysis based on linear elastic fracture mechanics (LEFM). In this type of analysis, the growth of an initial defect is calculated until the defect either penetrates the whole wall thickness of the component or the stress intensity factor reaches the critical value ( $K_{IC}$ ). To cover uncertainties in the analysis, three safety factors are applied: a) a factor of 2 on the initial defect area that can be detected; b) a factor of 2 on the number of fatigue life cycles; c) a factor of 1.5 (for normal operation conditions), on the value of  $K_{IC}$ .

#### *In-plane Loads at the Inboard Leg*

A 2D model of the TF coil at the inboard leg has been used for the analysis. This model includes details of the conductor and conductor insulation, the radial plates, the ground insulation and the case. The loads applied are the Lorentz forces acting on each conductor, and the poloidal tensile strains on the case and winding pack. These strains have been calculated with the global model described below. The Lorentz forces are reacted by the toroidal wedging pressure. Table 2.1.2-2 summarizes the main results of this analysis and, in particular, how the poloidal tensile and toroidal compressive forces are shared between the case and the winding pack. Figure 2.1.2-7 shows the stress intensity (Tresca) in the TF-coil casing and radial plates. All stresses are found to be within allowables.

**Table 2.1.2-2 Force and Stress at TF Inboard Leg**

Vertical force: - Winding pack - Case	(MN)	40 60	
Toroidal force: - Winding pack - Case	(MN/m)	- 60 - 82	
Maximum stresses in	Stress Type	Stress Value (MPa)	Allowables (MPa)
Case nose (at wedging surface)	$S_I$	665	
	$S_{tor}$	594	
	$P_m$	520	667
	$P_m+P_b$	670	867
Radial plates	$P_m+P_b$	701	867
Insulation (average shear)	$S_{xy}$	30	42*

$S_I$ : Tresca stress;  $S_{tor}$ : toroidal stress;  $P_m$ : primary membrane stress;  $P_b$ : bending stress;  $S_{xy}$ : shear stress; \*: shear stress allowable with > 36 MPa compression.

N 12 GR 648 01-05-30 W 0.1

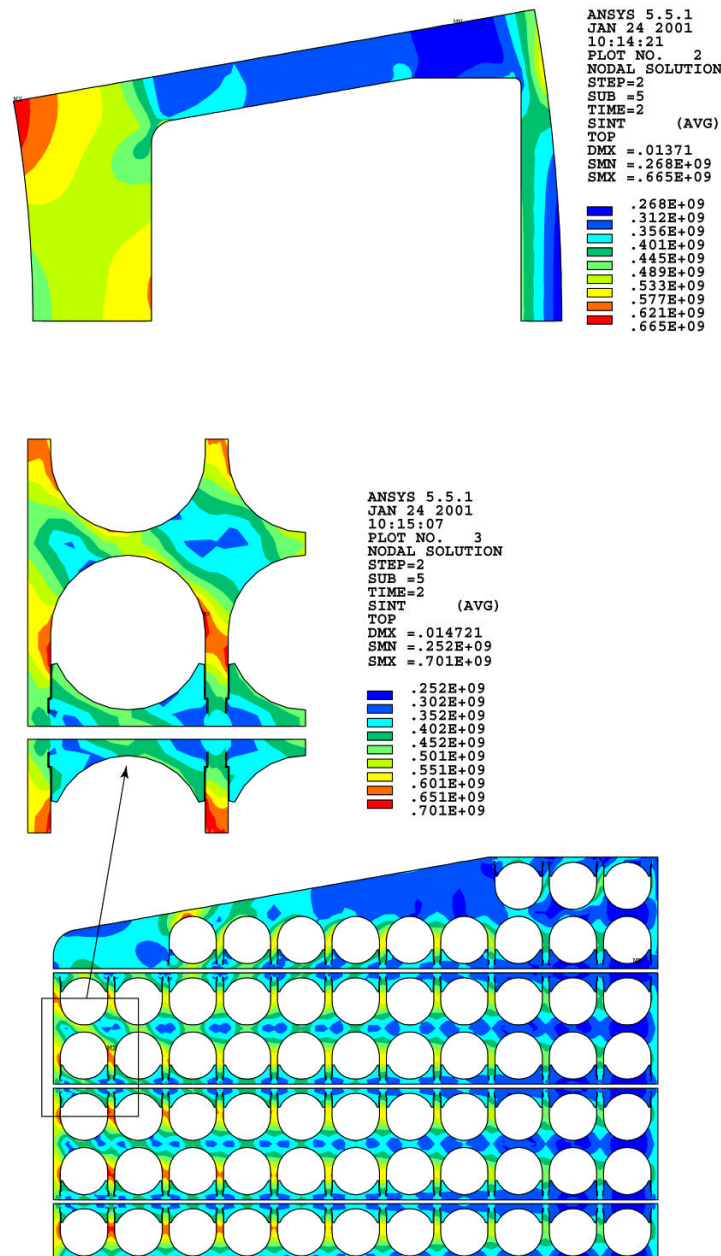


**Figure 2.1.2-7 Stress Intensity (Pa) in TF Coil Casing and Winding Pack Radial Plates in Inboard Region**

### *Global Stress Analysis of the TF Coils*

The global finite element model of the TF coils and structures is shown on Figure 2.1.2-8. The model incorporates the out-of-plane support structures and gravity supports. The pre-compression rings are not included but their effect has been simulated by local radial forces. The TF coil winding pack is represented by smeared material elastic properties. The model incorporates both in-plane and out-of-plane loads and the load cases considered include loading of the pre-compression rings at room temperature, TF magnet cool-down, TF magnet energisation, initial CS magnetization (IM) defined as the state when the CS is fully

energised just before plasma initiation, and end of burn (EOB). The scenarios considered are the reference 15 MA plasma scenario and a number of other scenarios including in particular the 17 MA plasma scenario.

N 11 GR 560 00-12-07 W 0.1

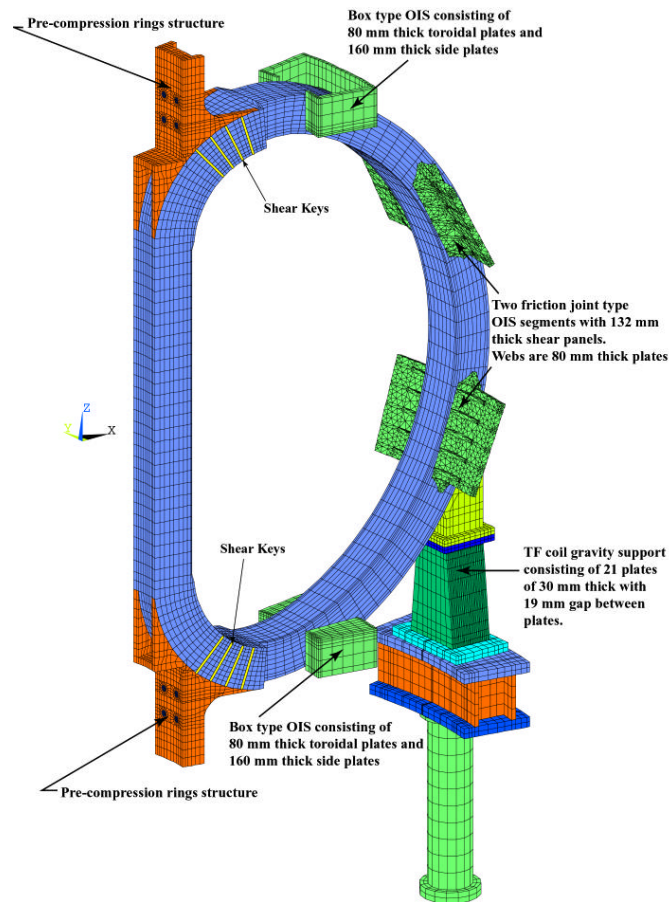


**Figure 2.1.2-8 Finite Element Model for TF Coil Analysis**

Critical regions have been identified at the upper and lower inboard curved regions where the coils are no longer wedged and behave as unsupported curved beams. In these regions, the out-of-plane forces peak and reverse direction (due to the presence of the PF1 and PF6 coils). These curved regions of the coil case have stress peaks located at the side walls at the end of the straight leg and in front of the shear keys.

Other critical regions are at the outboard legs in the vicinity of the intermediate OISs. Table 2.1.2-3 shows that the two intermediate OISs carry the bulk of the outboard leg shear loads associated with the TF coil overturning moment.

**Table 2.1.2-3 Shear Loads (MN) on OIS (15 MA, End of Burn)**

	<b>Radial shear</b>	<b>Vertical shear</b>
Upper OIS segment	1.1	1.55
Lower OIS Segment	0.73	1.83
	<b>Maximum shear</b>	
Upper intermediate OIS segment	22.7	
Lower Intermediate OIS segment	25.6	

These large shear loads generate bending moments and local stress in the case and OISs. Stress peaking occurs at the re-entrant corners where the OISs connect to the TF coil cases. These stress peaks have been mitigated by the use of large (500 mm) corner radii and local thickening of the structures. Such design features are compatible with a production of these parts by casting.

The fatigue analysis has been carried out assuming initial defects which are typical of the material and type of production (forgings and castings). A certain level of manufacturing residual stress has also been taken into account for forged sections and welds. Results are shown in Table 2.1.2-4 for the most critical locations. The allowable number of cycles shown in the table exceeds the required number of 60,000 (30,000 tokamak cycles with a safety factor of 2).

**Table 2.1.2-4 Fatigue Life in the TF Coil Case and OIS (15 MA Scenario)**

<b>Location</b>	<b>Type and area (mm<sup>2</sup>) of postulated initial defect</b>	<b>Allowable number of stress cycles</b>
Bottom of inboard leg, side wall	Sub-surface defect in forged base metal, 10 mm <sup>2</sup>	256,000
Bottom of inboard leg, side wall	Sub-surface defect in weld, 20 mm <sup>2</sup>	99,000
OIS panel (at attachment to case wall)	Sub-surface defect in cast base metal, 30 mm <sup>2</sup>	156,000

The results above are for a 15 MA plasma scenario. Analysis of the 17 MA scenario shows that the cyclic stresses tend to increase in proportion to the plasma current. The conclusion is that operation at 17 MA is possible but not for the full fatigue life (30,000 cycles) of the machine.

### 2.1.3 Conductor Design

#### 2.1.3.1 Conductor Design Criteria

The conductor design is governed by the three criteria of temperature margin, stability and hot spot temperature.

##### *Temperature Margin*

For Nb<sub>3</sub>Sn, the temperature margin, from the maximum predicted temperature at any point to the local (i.e. based on local peak field on the cable) current sharing temperature must be > 1K during plasma operation. In steady operation without plasma (i.e. in stand-by mode or

after a plasma disruption), the temperature margin must be  $> 0.5\text{K}$ . For NbTi, the temperature margin must be  $> 1.5\text{K}$ .

### *Heat Transfer to Helium and Stability*

The well-cooled, ill-cooled criterion, based on empirical assessments of coil performance, is used as a basis for the design with a heat transfer coefficient (which includes safety factors) of  $1,000\text{ W/m}^2\text{K}$  in Nb<sub>3</sub>Sn and  $600\text{ W/m}^2\text{K}$  in NbTi.

### *Hot Spot*

The maximum temperature that may be reached locally inside the conductor in the event of a quench has been determined by the differential expansion between conductor materials. Below 150K, materials have a low thermal expansion and 150K is therefore selected as the maximum temperature that may be reached by the conductor jacket. The cable inside the jacket may reach up to 250K on a transient basis as it is much more flexible than the jacket.

### 2.1.3.2 TF Conductor

The conductor is a circular Nb<sub>3</sub>Sn cable-in-conduit with a central cooling channel, cooled by supercritical helium. The TF conductor is almost identical to the conductor used for the TF model coil. As a result, the TF model coil development programme and manufacturing experience<sup>1</sup> are fully applicable, and have been used to establish the reference strand parameters (Table 2.1.3-1).

The conductor parameters are shown in Table 2.1.3-2 and the conductor design in Figure 2.1.3-1. The conductor current of 68 kA is determined by the geometrical fit of the conductors into the winding pack at the inboard leg, and the maximum allowable value of 70 kA.

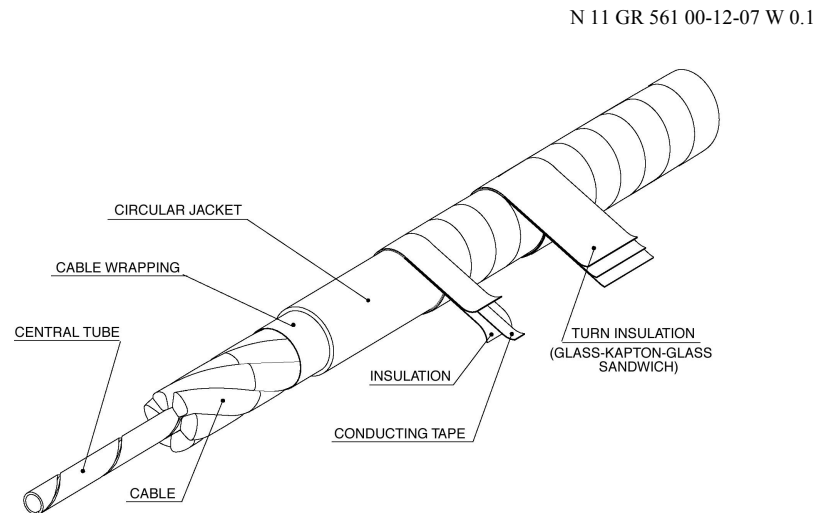


**Figure 2.1.3-1 TF Coil Conductor Design**

<sup>1</sup> K. Okuno, et al., "Key Features of ITER-FEAT Magnet System," 21st Symposium on Fusion Technology, Madrid, Spain, 11 - 15 September, 2000.

**Table 2.1.3-1 Nb<sub>3</sub>Sn Strand Properties for TF Coils and CS  
(Properties for a Superconductor Strain = - 0.25%)**

J <sub>c</sub> non copper at 12 T, 4.2K	650 A/mm <sup>2</sup>
B <sub>com</sub>	28 T
T <sub>com</sub>	18K
T <sub>c</sub> at 12 T	11.7K
Hysteresis loss (± 3 T cycle)	400 mJ/cm <sup>3</sup> of non-copper

**Table 2.1.3-2 TF Conductor Parameters**

Coolant inlet temperature	4.6K
Operating current (kA)	68.00
Nominal peak field (T)	11.8
Operating temperature (K)	5.0
Operating strain (%)	- 0.5
Equivalent discharge time constant (s) hot spot	15
Current sharing temperature (K)	6.03
I <sub>operation</sub> /I <sub>critical</sub> at 5.0K	0.765
Cable diameter (mm)	40.2
Central spiral outer diameter x inner diameter (mm)	8x6
Conductor outer diameter (mm)	43.4
Jacket material	steel

The strands, about 0.7 mm in diameter, are cabled to a 5 stage cable with the final 6 fifth-stage subunits cabled around a central cooling spiral. The local cable space void fraction is about 34%, to give an acceptable level of transverse conductivity. The cable incorporates pure copper strands to build up the copper section necessary for quench protection, and the final substage has a 50% wrap of Inconel foil (0.1 mm thick) to control AC losses. The final cable is jacketed by the pull-through method with a circular stainless steel tube. The use of stainless steel matches the thermal contraction of the radial plate and avoids delamination of the radial plate insulation layer that occurs over the cover of the conductor groove if a jacket having a significantly different thermal contraction coefficient is used.

The size of the central channel and cooling flow rate (8 g/s per channel) are essentially determined by the nuclear heat. With the reference strand and cable configurations (the cable coupling time constant is assumed to be 50 ms), AC losses in the winding pack during plasma operation are low compared to the nuclear heating and do not represent a design constraint, as shown in Table 2.1.1-5. Although experimental results from the CS model coil programme<sup>1</sup> indicate that coupling losses could be higher, with a coupling time constant of 100 - 200 ms, this would not require a modification of the TF coil conductor design.

The cooling inlets to each pancake are located at the inner surface of the coil. The cold helium then reaches the high field region and, after passing through the pancake, exits on the

<sup>1</sup> H. Tsuji, et al., "Progress of the ITER Central Solenoid Model Coil Program," 18th IAEA Fusion Energy Conference, Sorrento, Italy, 4 - 10 October, 2000.

outer surface of the coil on the outside. The conductor design point of maximum field and maximum temperature occurs towards the end of the TF coil inboard leg, where the helium in the first turn reaches the maximum temperature due, essentially, to the nuclear heat at the inboard leg (where the shielding is thinnest).

### 2.1.3.3 CS Conductor

The superconductor for the CS is a Nb<sub>3</sub>Sn cable-in-conduit type, almost identical to the conductor used for the CS model coil<sup>1</sup> and, therefore, the CS model coil development programme and manufacturing experience are fully applicable. Several design options are being considered for the CS conductor (see 2.1.5.1). In this section, only the design with an extruded square jacket is described.

The conductor current is chosen to be in the range 40 - 46 kA as a compromise between structural issues (the larger the conductor, the larger the stress concentration factors on the jacket), and cable current density (the larger the current, the lower the amount of copper required for thermal protection). The conductor jacket is thick, with a square outer section, and is made of Incoloy 908 or stainless steel, to provide the main structural support for the CS.

The conductor parameters for the Incoloy and steel options are summarised in Table 2.1.3-3 for each of the 6 modules forming the CS stack. The conductor has two design conditions. At IM, the CS modules are all energised with a similar current to a peak field of 13.5 T. This field is achieved with a conductor current of 41.8 kA. At EOB, the current is concentrated in the central CS modules, and the plasma and PF coils act to reduce the overall field. The result is that the peak field is set lower, at 12.8 T, but also that a higher current, 46 kA, is required to reach this. The conductor design is a compromise between these two operating conditions. The cable configuration is similar to that used for the TF coil conductor, with 6 sub-cables arranged around a central cooling space.

The modules are wound as hexa-pancakes and quad-pancakes (see 2.1.5.2) with the helium inlet at the inner diameter in the cross-over regions and the outlet at the cross-over regions at the outer diameter. The high field region is therefore cooled by the coldest helium.

---

<sup>1</sup> H. Tsuji, et al., "Progress of the ITER Central Solenoid Model Coil Program," 18th IAEA Fusion Energy Conference, Sorrento, Italy, 4 - 10 October, 2000.

**Table 2.1.3-3 CS Conductor Parameters (Incoloy or Steel Square Jacket)**

	<b>Incoloy Square Jacket</b>	<b>Steel Square jacket</b>
Coolant	Inlet 4.65K	Inlet 4.65K
Type of strand	Nb <sub>3</sub> Sn	Nb <sub>3</sub> Sn
Operating current (kA) IM/EOB	41.8 / 46.0	41.8 / 46.0
Nominal peak field (T) IM/EOB	13.5 / 12.8	13.5 / 12.8
Operating temperature (K)	4.7	4.7
Operating strain (%)	- 0.15	- 0.50
Equivalent discharge time constant (s)	11.5	11.5
Tcs (Current sharing temperature) (K) @ 13.5 T	5.8	
Iop/Ic (Operating current/critical current) IM	0.774	0.735
Cable diameter (mm)	31.8	33.2
Central spiral outer x inner diameter (mm)	8x6	8x6
Conductor outer dimensions (mm)	49.5x49.5	49.5x49.5
Jacket material	Incoloy 908	Stainless steel

#### 2.1.3.4 PF Conductor

The PF coils use NbTi superconductor, cooled by supercritical helium. This gives a substantial cost saving compared to Nb<sub>3</sub>Sn, and the elimination of a reaction heat treatment greatly simplifies the insulation of such large diameter coils.

The conductor design criteria (1.5K, 600 W/m<sup>2</sup>K and 150K) are slightly different to Nb<sub>3</sub>Sn (the temperature margin is higher) because of the lower critical temperature of NbTi. The reference strand parameters are given in Table 2.1.3-4.

**Table 2.1.3-4 NbTi Strand Parameters**

J <sub>c</sub> non-copper at 5 T, 4.2K	2,900 A/mm <sup>2</sup>
T <sub>c</sub> at 5 T	7.17K
Filament diameter	5 μm
Strand layout	no CuNi internal barriers, Nickel surface coating

The cable configuration is similar to that used with Nb<sub>3</sub>Sn with 6 sub-cables arranged around a central cooling space. The conductor current is chosen in the range 40 - 45 kA because of the similarity with the CS conductor and the R&D database. No advantage has been found in using higher current conductors, as the copper fraction is limited by stability. The conductor design is shown in Figure 2.1.3-2.

N 12 GR 32 00-12-07 W 0.1

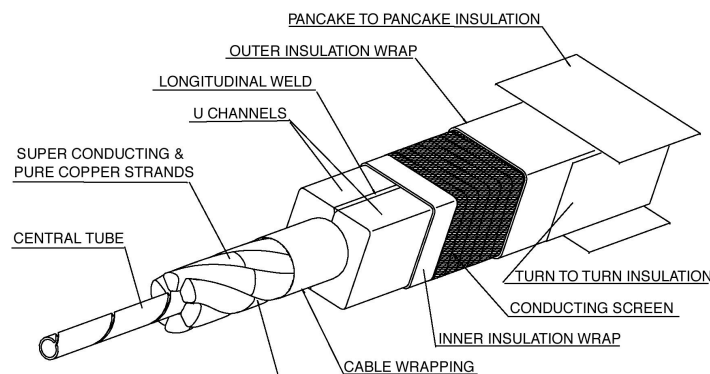


**Figure 2.1.3-2 PF Coil Conductor Design**

Non-uniform current distribution can be a more sensitive issue with NbTi cables than with Nb<sub>3</sub>Sn cables because of the lower value of the critical temperature  $T_c$ . To ensure a uniform current distribution in each sub-cable while maintaining AC losses at an acceptable level, the transverse resistivity within the cable must be controlled. A coating (nickel is the reference candidate) is used on the strands. Coupling currents are controlled by the Inconel wrap on each sub-cable to limit the coupling time constant to about 50 ms and the joint layout must provide a uniform contact to each of these sub-cables.

The PF conductors are designed with the capability to operate at a higher current to compensate for the loss of one double-pancake, while still maintaining the same total current capacity in each coil. This mode of operation is referred to as 'backup mode' in 2.1.6.1. In such a case, not only the conductor current increases but also the peak field. Three different conductor designs corresponding to three field values have been selected for the PF conductor design. For the PF2, 3 and 4 coils, the field is up to 4 T, for the PF5 coil, up to 5 T and for the PF1 and 6 coils, up to 6 T. These conductors are shown in Table 2.1.3-5. Both normal mode and backup mode operations can be achieved within the field limits for the 2 lower grades, while the operating field upper limit of the high grade is increased up to 6.4 T in backup mode and requires an operating temperature of 4.7K instead of 5K (sub-cooling is required with the coil He inlet at 4.4K instead of 4.7K).

**Table 2.1.3-5 Types of PF Conductor**

Coils	Design Current (kA), Peak Field (T), Operating Temperature (K)	
	Normal mode	Backup mode
PF1 & PF6	45.0 kA, 6.0 T, 5.0K	52.0 kA, 6.4 T, 4.7K
PF2, 3 & PF4	45.0 kA, 4.0 T, 5.0K	52.0 kA, 4.0 T, 5.0K
PF5	45.0 kA, 5.0 T, 5.0K	52.0 kA, 5.0 T, 5.0K

The conductor parameters are shown in Table 2.1.3-6. The selected operating temperatures include a 0.3K temperature increase (due mainly to AC losses) at the maximum field within the coil, and assumes an inlet temperature of less than 4.7K, allowing a cryoplant window of 4.4 - 4.7K for the PF coils. The helium mass flow per channel is 10 g/s.

**Table 2.1.3-6 PF Conductor Parameters**

Parameters	PF1 & 6	PF2, 3 & 4	PF5
Coolant inlet temperature (normal/backup)	4.7K /4.4K	4.7K	4.7K
Operating current (kA) (normal/backup)	45 / 52	45 / 52	45 / 52
Nominal peak field (T) (normal/backup)	6.0 / 6.4	4.0	5.0
Operating temperature (K) (normal / backup)	5.0 / 4.7	5.0	5.0
Equivalent discharge time constant (s) hot spot	18	18	18
Current sharing temperature (K) (normal/backup)	6.5 / 6.27	6.65 / 6.51	6.60 / 6.51
$I_{\text{operation}} / I_{\text{critical}}$ (normal/backup)	0.127 / 0.144	0.365 / 0.422	0.264 / 0.305
Cable diameter (mm)	38.2	34.5	35.4
Central spiral outer x inner diameters (mm)	12x10	12x10	12x10
Conductor outer dimensions (mm)	53.8x53.8	52.3x52.3	51.9x51.9

The conductors use a heavy-walled, stainless steel jacket. Two jacket options are being considered:

- i) the reference option: extruded circle-in-square steel conductor;
- ii) the alternative option: thin steel circular jacket with external steel U-channels.

In each case, the cable is placed in the jacket by a pull-through, roll-down procedure, as with the TF and CS coils. The U-channels are welded around the circular jacket before spooling. The external shape of these two conductor options is the same and the choice has no impact on the PF coil manufacture, except for the preparation of helium inlet pipes and conductor joints and terminations.

#### 2.1.3.5 CC Conductor

The CCs use a 10.0 kA cable-in-conduit conductor using NbTi superconductor. This CC cable is conservatively designed to operate up to 6 T and 5K. It is formed square with a square outer jacket. The main parameters are summarised in Table 2.1.3-7.

**Table 2.1.3-7 Conductor Parameters for the Correction Coils**

Operating current (kA)	10.0
Nominal peak field (T)	6.0
Operating temperature (K)	5.0
Jacket material	Cold-worked 316LN

#### 2.1.4 TF Coils Manufacture

The 18 TF coils are each D-shaped and consist of a winding pack contained in a thick steel case. The winding pack is a bonded structure of radial plates (which contain the conductor) with an outer ground insulation.

### 2.1.4.1 TF Coil Winding Pack

The winding pack design is based on the use of circular conductors supported by radial plates, as shown in Figure 2.1.4-1. This design has advantages in terms of the conductor insulation, long-term quality, and reliability.

N 11 GR 562 00-12-07 W 0.1

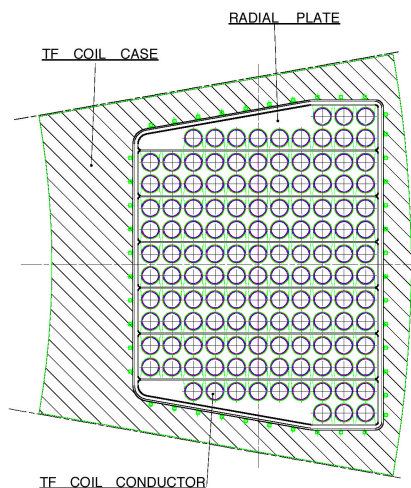


**Figure 2.1.4-1 Cross Section of TF Coil at Inboard Leg**

- A circular outer cross section of the jacket is the optimum shape for applying insulation tapes, resulting in a robust turn insulation. The turn insulation is not subject to the stress concentration effects which are always present at corners of square conductors.
- During the magnet operation, the Lorentz forces acting on each conductor are transferred to the plate, without accumulation of forces on the conductor and its insulation. As a result, almost no primary load is applied to the conductor insulation and there is no degradation leading to damage due to mechanical cycling.
- With circular conductors in radial plates, delamination between the conductor insulation and the radial plate is of no consequence and has no impact on the mechanical or electrical behaviour of the winding pack.

Additional advantages of the radial plate configuration are that it provides a “double insulation” with two physically independent barriers (the turn and the ground insulation) and it gives the capability of detecting impending faults by monitoring the resistance between conductor and radial plate.

The considerations above indicate that with the radial plate configuration, faults leading to a TF coil short are essentially avoided by design. The radial plate concept has already been demonstrated in the TF model coil project. The main drawback, however, is the relatively high manufacturing cost of the radial plates. R&D activities have been initiated to investigate potentially cheaper manufacturing routes.

The winding uses one-in-hand conductor (about 800 m long) with a double pancake configuration. The conductors are wound and heat treated (about 650°C for 200 hrs) in a vacuum furnace. After heat treatment, the turn insulation is applied. The insulation consists of a polyimide/glass-fibre mix with epoxy resin filler. The insulated TF conductors are then

placed in grooves on each side of a radial plate. Each conductor is contained in its groove by means of a cover plate that is welded in place.

Seven double pancakes are assembled together to form the winding pack of one TF coil. The ground wrap has a minimum thickness of 6 mm and includes multiple wraps of polyimide tape interleaved with glass, vacuum impregnated with epoxy resin. The joints are placed outside the main winding (in a “praying hands” configuration). The coil terminals project out of the case on the lower curved part of the case.

#### 2.1.4.2 TF Coil Cases

The TF coil cases are composed of two half-cases made up of about 7 poloidal sections. These sections are joined by butt welds which have been located, as far as possible, outside the peak stress regions (in particular the upper and lower inner curved regions). The final weld to close the half cases around the winding pack (which cannot be inspected from both sides) is located on the coil midplane where the cyclic stress component is a minimum (Figure 2.1.4-2).

N 11 GR 563 00-12-07 W 0.1

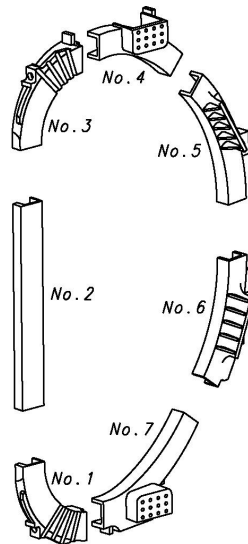


**Figure 2.1.4-2 Proposed Segmentation of the TF Coil Case for Manufacture**

The high stress sections of the case (the inboard leg and upper and lower inboard curved regions) can be made from high strength forged 316LN (modified) steel. This can be forged avoiding any intermediate welds to build the half case section. On the outboard part of the coil, cast sections have lower stress limits but greatly reduce the amount of welding and appear the most attractive design solution. Butt welds between poloidal sections are expected to be a combination of electron beam welding for the first pass followed by multiple passes of submerged arc welding for the remainder.

The cases are equipped with a set of cooling channels to intercept nuclear and eddy current heat loads before they reach the superconductor in the winding pack. These channels are placed on the inner surface of the case and run poloidally around the circumference (Figure 2.1.4-1).

## 2.1.5 Central Solenoid Manufacture

### 2.1.5.1 Flux Generation and Conductor Jacket Options

The solenoid is free-standing and supports the magnetic loads through structural material within the winding. The main load is the magnetic hoop force, which creates tension in the structural material. Because of its central position in the tokamak, the CS has a major role in driving the radial build while itself forming a fairly minor fraction of the total magnet cost (about 12%). Global optimisation studies have shown that in order to minimize the total cost of the machine, it is preferable to adopt the most compact, high field design option, even if it is not the lowest cost choice for the CS itself. As illustrated in Figure 2.1.5-1, the flux generation in the solenoid is improved by the choice of a high field and the use of the highest allowable tensile stresses in the jacket material. For ITER, a peak field of 13.5 T and a tensile peak stress of about 410 MPa have been selected to meet the flux generation requirements.

N 13 GR 27 00-12-07 W 0.1

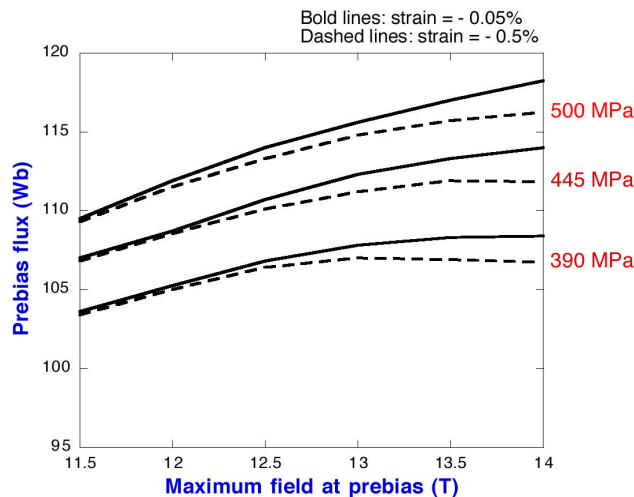


**Figure 2.1.5-1 Pre-bias Flux Available from an Optimised CS as a Function of Field, Showing Variation with Allowable Peak Tension and Superconductor Strain**

The requirements for the CS conductor jacket material are, therefore, primarily a high fatigue resistance to stress cycling.

There are two basic design options for the CS jacket, as shown in Figure 2.1.5-2, both of which are expected to provide the same flux capability.

- i) An extruded jacket with a square outer section. The jacket material is subjected to the Nb<sub>3</sub>Sn heat treatment. The possible jacket materials are Incoloy 908, as developed for the CS Model Coil, or a stainless steel, once such a steel has been developed to meet the fatigue life requirements after heat treatment.
- ii) A double jacket including an inner titanium circular jacket, which undergoes the Nb<sub>3</sub>Sn heat treatment, and an outer stainless steel jacket made up of two U-channels which are applied around the inner jacket after the heat treatment.

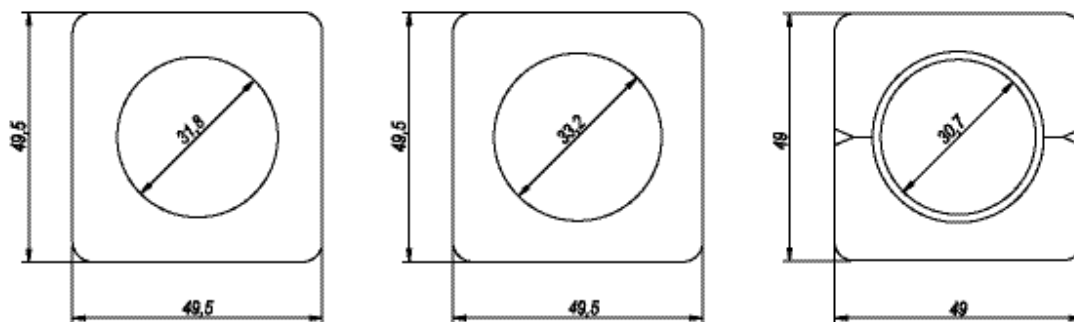


**Figure 2.1.5-2 CS Conductor Jacket Options**  
**Incoloy 908 (left), Stainless Steel (center), Double Jacket (Ti-SS) (right)**

Incoloy 908 has significant advantages in terms of its very high fatigue resistance and its thermal contraction which matches that of  $\text{Nb}_3\text{Sn}$ . The use of Incoloy has been successfully demonstrated in the CS model coil. Incoloy 908 is, however, sensitive to stress-accelerated grain boundary oxidation (SAGBO) during the  $\text{Nb}_3\text{Sn}$  heat treatment, and requires strict control of the heat treatment atmosphere ( $\text{O}_2 < 0.1$  ppm).

There has been recently significant progress in the development of stainless steel as a jacket material for the CS. Solution annealing has been shown to improve the fatigue behaviour (crack growth rate) of those steels. At the time of writing this report, the improvement in property is, however, not quite sufficient to meet the ITER CS fatigue life requirements. It is concluded that the use of steel will become possible only if further improvements of the fatigue behaviour can be achieved or if the detection sensitivity of certain defects (sub-surface defects) can be improved. The planned R&D programme includes the study of vacuum-refined materials and this may result in further improvements.

The double jacket option does not require such strict control procedures for the reaction treatment. For this option, JK2 is proposed as the material of the outer jacket. This material is a cryogenic steel developed in Japan and has a coefficient of thermal contraction close to that of  $\text{Nb}_3\text{Sn}$  between room temperature and 4K. However, JK2 in extruded sections is not fully characterised at cryogenic temperature, especially for fatigue properties. R&D activities are underway to demonstrate the manufacture of U-channels and to establish the fatigue properties of JK2. Some additional work on the use and joining of titanium is also probably required. The main drawback of the double jacket option is the relative complexity of the assembly of the U-channels on the reacted conductor. R&D would be required to fully establish the assembly procedures.

Incoloy 908 is maintained, at present, as the provisional reference solution. The possibility to use stainless steel is very attractive and will be kept under review as new R&D results become available. The Ti-JK2 option remains as alternative solution but requires additional R&D. The final choice will be based on the R&D results.

#### 2.1.5.2 CS Winding Pack

The CS stack consists of 6 electrically independent modules. The modules are each made up of 5 “hexa-pancake” and 2 “quad-pancake” windings (a “hexa-pancake” and a “quad-pancake” use a single conductor length for the winding of 6 pancakes and 4 pancakes

respectively). The electrical joints between hexa or quad pancakes are located at the CS outer diameter and are embedded in the winding pack. Each module weighs about 107 t.

A previous CS jacket design used a smaller extruded section with a co-wound reinforcing strip. The main advantage of this design was to reduce the cross sectional area of the butt welds joining the jacket lengths. However, the co-wound strip complicates the winding process and either requires a longitudinal weld to the square jacket or, if not welded, requires additional insulation which reduces the current density. The single square section is therefore preferred.

Insulation is applied after the conductor is reacted. The turn insulation is applied to the conductor and the strip and consists of overlapping glass and polyimide tapes. Additional insulating shims (1.5 mm thick) are inserted between turns and between pancakes to compensate dimensional deviations of the conductor. To make the joints between the hexa-pancakes, the conductor ends are pulled into an helical shape to provide access to the joint area between two adjacent hexa-pancakes. After stacking all hexa-pancakes, the ground insulation (10 mm thick of overlapping glass and polyimide tapes) is applied. The whole CS module is then subjected to a final vacuum pressure impregnation (VPI) process with epoxy resin.

### 2.1.5.3 CS Preload Structure

The field curvature at the ends of the CS stack creates vertical forces on the modules. At IM (initial magnetization), these forces are towards the mid-plane of the stack, whereas at EOB (end of burn), the end modules carry opposite currents to the central ones and are repelled with a force up to 75 MN. This means that a vertical support structure is required. This structure applies axial pre-compression to the coil stack so that the modules remain in contact during all operating conditions (Figure 2.1.5-3).

N 13 GR 29 00-12-07 W 0.1

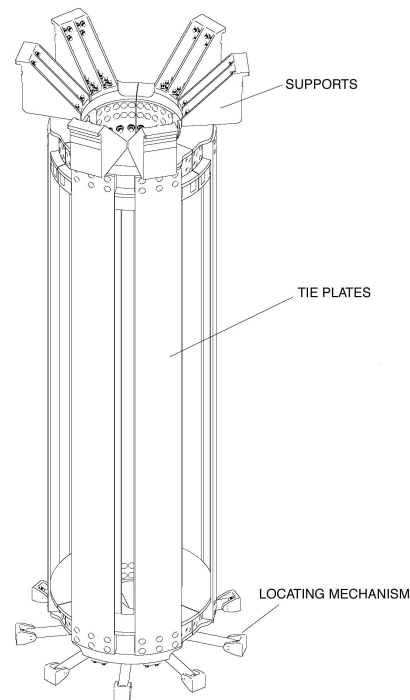


**Figure 2.1.5-3 CS Supports and Pre-load Structure**

To obtain uniform compression, tie plates running axially along the CS are provided at both inside and outside diameters and connect to rigid flanges at top and bottom. This structure is designed so that it can restrain the maximum vertical separating load. The required axial tension in the structure is achieved partly by pre-tensioning at room temperature and partly by differential contraction during cooldown. This approach relies, therefore, on the use of a jacket material with a thermal contraction coefficient lower than that of the tie-plates. The combination of Incoloy as a jacket material and stainless steel for the tie-plates provides the required differential contraction. If the case of a stainless steel jacket material, preliminary analysis has shown that aluminium tie-plates can provide the required vertical pressure. A full design and analysis of aluminium tie-plates remains, however, to be performed.

The CS pre-load structure consists of the lower flange, the upper flange, buffer plates, a set of 12 tie-plates together with wedges and connecting bolts. The flanges are split into 12 sectors linked by electrically insulated bolted joints to reduce AC losses during pulsing of the machine. The tie plate region needs to have at least 30% open space in the toroidal direction for the current lead and helium pipe arrangement.

The CS assembly is hung from the top of the TF coils through its pre-load structure by supports which resist the net vertical forces but are flexible in the radial direction. At the bottom of the CS, there is a locating mechanism to support the stack against dynamic horizontal forces.

#### 2.1.5.4 CS Joints and Helium Pipe Inlets

The CS joints between hexa-pancakes are located at the outer diameter. Two types of joints are being considered: the overlap type and the butt type. The overlap type of joint uses a cable compacted into a long (typically 500 mm) tube or box with a copper wall to achieve low contact resistance. Contact is achieved by clamping together the two conductor tubes or boxes. In the butt joint, the cable is highly compacted into a copper tube and cut normal to the conductor axis to allow a sintered joint to be made between the two conductor ends. These two joint concepts have been used in the CS model coil and the choice will be made when all experimental data on joint performance has been analysed.

For both types of joint, a structural element, composed of an extension of the reinforcing strip, is provided to transfer the operating hoop load on the conductor around the joint region.

On the top and bottom modules, the joints are exposed to a significant transverse (i.e. radial) field component during plasma operation. This field variation is unfavourable for the "overlap" type of joint since it drives eddy currents in a loop through the joint contact surface. Testing of overlap joints in this configuration is required.

Helium inlets are at the CS inner diameter where tensile stresses are highest. The helium inlet region requires, therefore, a local reinforcement to allow the opening in the conductor jacket without excessive stress intensification. The inlet must also provide a good distribution of helium in the 6 sub-cables of the conductor. These requirements are achieved by cutting locally the jacket and welding specially shaped L-shaped pieces, which include the helium inlet channel, together with the required structural reinforcements and interspace to distribute the helium flow.

### 2.1.5.5 CS Structural Assessment

The main loads are the magnetic hoop force, which creates hoop tension in the structural material, and the vertical pressure towards the equatorial plane from the outer modules, which creates vertical compression. Analysis of the CS includes global and detailed analysis. Global analysis has been carried out to investigate the behaviour of the CS stack and pre-load structure during the operation scenario. This type of analysis uses models where the CS windings are represented by smeared material elastic properties. A 2D axisymmetric model and a 3D model to look at non-axisymmetric aspects of the windings and structures have been used. Detailed analysis of the CS winding structure has been carried out to evaluate the detailed stress distribution in the conductor and its insulation. This analysis has been carried out with 2D axisymmetric models.

The key parameter is the fatigue strength, which determines the allowable peak tensile stress in the jacket. The highest stresses occur at the inner diameter of the CS. The stress pattern depends on the geometrical configuration of the conductors. The worst configuration is where conductors in neighbouring pancakes are vertically staggered due to turn to turn transitions within pancakes. In this worst configuration, peak tensile stress occurs in the horizontal wall of the conductor jacket. This peaking is due partly to bending of the conductor wall (under the axial pressure) and partly to differential Poisson effects. Table 2.1.5-1 summarizes the main results of the stress analysis and fatigue assessment. For the CS, each plasma cycle includes two stress cycles: one full stress cycle at IM and a cycle at reduced stress at EOB. For the stainless steel option, the stress level is about 10% higher than for the Incoloy option due to the higher differential contraction which reduces strand performance and requires, therefore, a larger cable cross section. A certain level of manufacturing residual stress in the jacket has also been taken into account in the fatigue assessment. The maximum allowable initial defect areas are shown in the table. For the Incoloy option, the defect size is within the sensitivity of non-destructive testing techniques. For the stainless steel option, the defect size is smaller and may be outside the detection capability of non-destructive testing techniques.

**Table 2.1.5-1 Tensile Stress in the CS Conductor Jacket and Acceptable Defect Size for the Incoloy and Stainless Steel Square Jacket Options**

<b>Conductor option</b>	<b>Peak tensile stress in the jacket (MPa) IM / EOB</b>	<b>Maximum allowable initial defect* area (mm<sup>2</sup>) to achieve 60,000 plasma cycles</b>
Incoloy	429/401	0.65
Stainless steel**	470/440	0.28

\* A sub-surface defect is assumed.

\*\* The material is a solution heat treated, unaged 316LN steel.

The conductor turn insulation is subject to some shear stress and tensile stress normal to the insulation layer. These stresses are due to bending deformations of the conductor jacket under the axial pressure. Analysis shows that these shear stresses are acceptable but tensile stresses exceed locally the allowable limits. This effect, which was already present in the 1998 CS design, has been investigated experimentally by the US Home Team. A beam representing a section of the winding pack was tested under cyclic compressive load. Local delamination of the insulation near the corners of the conductors was observed, as expected, but without any adverse consequence for the integrity of the electrical barrier of the conductor insulation.

## 2.1.6 PF Coils Manufacture

### 2.1.6.1 PF Winding Packs

The PF coils are pancake wound with NbTi superconductors in square jackets. Because of the operational reliability requirements, especially for the electrical insulation, and the difficulty in replacing a coil, the conductor is provided with double turn insulation. The double turn insulation consists of two insulation layers with a thin metal screen in between. Double pancakes are wound two-in-hand. This arrangement allows detection of an incipient short, before it develops into a full short resulting in significant damage to the coil and, as a consequence, the need for a major coil repair or replacement. In the event of the detection of an incipient short in a double pancake, the faulty double pancake must be disconnected and by-passed using busbar links. This work is to be carried out hands-on and requires access to the joint regions at the outer diameter of the coils. Following the by-pass of a double pancake, plasma operation can continue at full performance by using the remaining double pancakes at higher current (backup mode).

The use of double turn insulation and the ability to continue operation with a by-passed double pancake should make a major coil repair or replacement unnecessary throughout the life of ITER-FEAT.

Should, however, such major repair be required, the following strategy could be followed:

- the upper coils, PF1 and PF2, can be relatively easily removed from the cryostat - for them, major repair work, or rewinding, should be carried out outside the cryostat;
- for the lower coils, PF5 and PF6, major repair work, including rewinding, should be carried out under the machine inside the cryostat;
- the PF3 and PF4 coils are trapped by the vacuum vessel ports and are the most difficult to access and repair; for this reason, their resistance to faults has been enhanced by using double pancakes with individual ground insulation and steel separator plates between double pancakes to limit damage propagation in the event of a fault.

Figure 2.1.6-1 shows typical PF coil cross sections. In the PF1, 2, 5 and 6 coils, the outer surfaces of the whole coil are covered with ground insulation with a thickness of 8 mm. The insulation is composed of overlapping glass and polyimide film (barrier) and is vacuum pressure impregnated with epoxy resin. In the PF3 and 4 coils, the outer surface of each double-pancake is covered with ground insulation with a thickness of 8 mm. A steel separator plate is placed between two double pancakes. The plate is formed from a steel strip with a spiral shape so as to form a flat pancake to reduce eddy currents.

N 12 GR 33 00-12-07 W 0.1

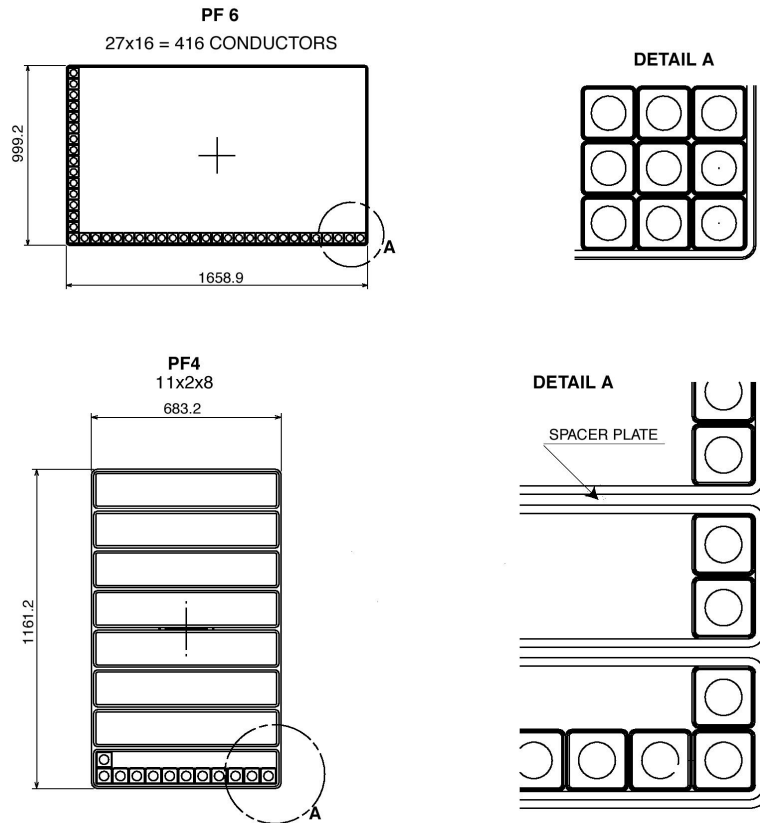


**Figure 2.1.6-1 PF Coil Typical Cross Sections**

### 2.1.6.2 PF Joints and Helium Pipe Inlets

The conductors at the ends of each double pancake are brought out of the winding at the outer diameter of the coil. The lap joint is made in the toroidal direction and a structural element is provided to transfer the operating hoop load on the conductor around the joint area. Each double pancake is to be supplied with supercritical helium at the inner diameter of the coil through a coolant inlet pipe located at the cross-over region of each of the two conductors.

### 2.1.7 **Correction Coils Manufacture**

Eighteen multi-turn correction coils (CCs) are used to compensate field errors arising from misalignment of the coils and winding deviations from the nominal shape as a result of fabrication tolerances, joints, leads, busbars and assembly tolerances. There are 6 top CCs, 6 bottom CCs, and 6 side CCs, arranged toroidally around the machine inside the PF coils. Pairs of diametrically opposite CCs are connected in series inside the cryostat.

The top and bottom coil sets are essentially planar while the side coils lie on a cylindrical surface. Each coil consists of a bonded winding pack enclosed in a 20 mm thick steel case. The vertical sections of each coil are placed to coincide with a TF coil leg and the coils are supported by clamps attached to the TF coil cases. The layout and geometry of the CCs is shown in Figure 2.1.7-1.

N 12 GR 34 00-12-11 W 0.1

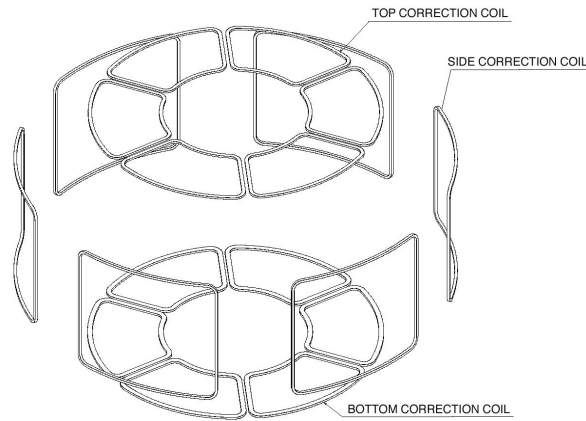


**Figure 2.1.7-1 Correction Coils Layout**

The current capacity of the CCs is shown in Table 2.1.7-1.

**Table 2.1.7-1 Operating Condition of the Correction Coils**

Parameters	Top coil	Side coil	Bottom coil
Max. operating current (kA)	10.0	10.0	10.0
Max. current capacity per coil (kA)	140	200	180
Max. total field (T)	< 6	< 6	< 6

## 2.1.8 Auxiliary Systems

Magnet feeders include the in-cryostat feeders, the cryostat feedthroughs, and the coil terminal boxes or structure cooling valve boxes.

### 2.1.8.1 In-cryostat Feeders

Each in-cryostat feeder is a subassembly that connects a coil or structure to the end of a cryostat feedthrough (CF) located at the cryostat wall. For a coil, it consists of a steel conduit containing the feed and return busbars (using NbTi superconductor), the return and supply helium lines and high and low voltage instrumentation lines. Figure 2.1.8-1 illustrates, as an example, the layout of magnet feeders at the lower part of the cryostat. The figure shows the feeders from their respective coil terminals inside the cryostat to the coil terminal boxes in the gallery of the tokamak building.

N 11 GR 565 00-12-07 W 0.1

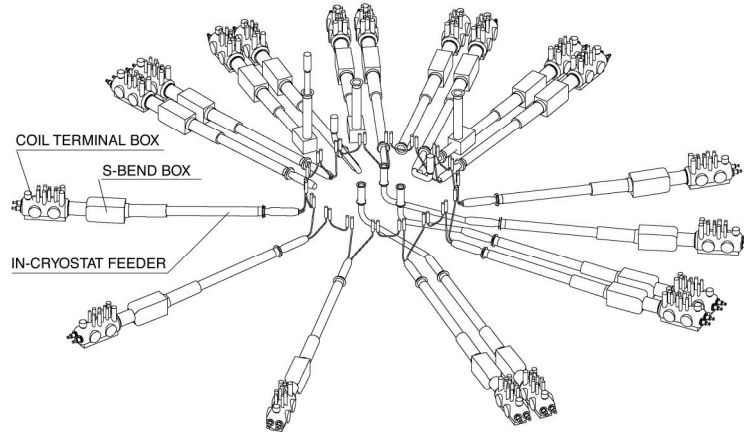


**Figure 2.1.8-1 Layout of Feeders at the Lower Part of the Cryostat**

Each busbar has a double insulation system that will allow detection of a developing busbar-to-ground short circuit and allow operation to be stopped before the short occurs, providing protection against further damage. Additionally, an over-wrap of steel tape will be applied to serve as an extra protection screen against a short circuit between coil terminals. In each feeder, the pair of superconducting busbars is separated by a steel plate acting as an additional robust protection against damage propagation between busbars. Figure 2.1.8-2 shows the typical design of a feeder joint and the details of the joints between a coil terminal and the feeder.

N 11 GR 566 00-12-07 W 0.1

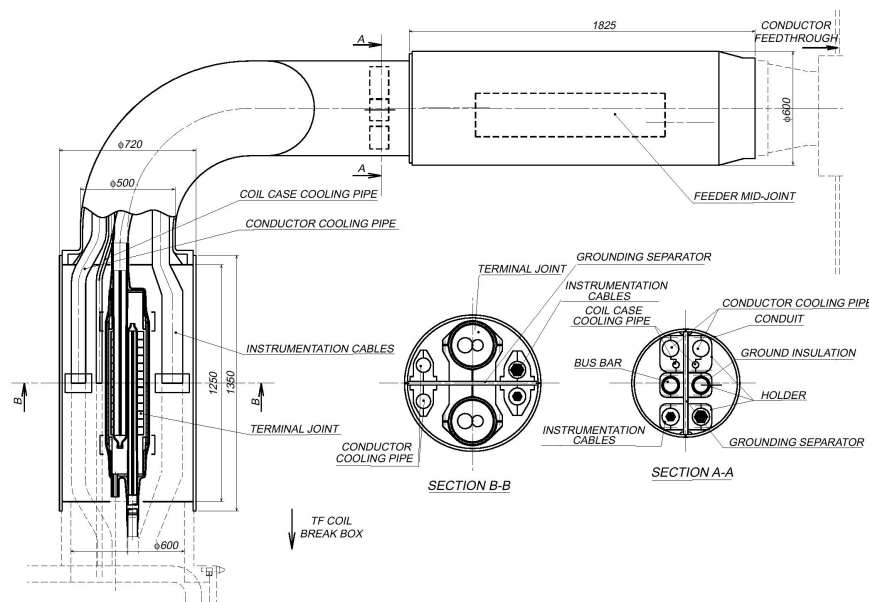


**Figure 2.1.8-2 Typical Terminal Joint and Feeder Cross Section**

The superconducting cable for the busbars is designed to have more thermal protection than the coils, so that the coils can still be properly discharged in the event of a busbar quench. The time constant of the current decay is taken as 26 s, approximately twice that of the coils. The operating current is taken as 68 kA for all coils, which provides some over-capacity for the CS and PF coils busbars. This has a negligible cost impact and allows a standard cable design. Table 2.1.8-1 shows some of the busbar conductor specifications.

**Table 2.1.8-1 Superconducting Conductor for TF, CS and PF Coil Busbars**

Type of strand	NbTi
Operating current (kA)	68
Nominal peak field (T)	4
Operating temperature (K)	5.0
Equivalent discharge time constant (s) hot spot	26
Cable diameter (mm)	41
Central spiral od x id (mm)	8x6
Conductor OD (mm)	47
Jacket	steel

#### 2.1.8.2 Cryostat Feedthrough

The cryostat feedthrough (CF) includes the penetration through the cryostat wall and a straight length from the cryostat wall to an S-bend box. The S-bend box is also part of the CF and contains S-shaped bends in the busbars and the cooling lines so as to accommodate the movements of the in-cryostat feeders and the coils, relative to the S-bend boxes which are fixed to the building.

The S-bend box connects to a coil terminal box (CTB). The vacuum barrier at the flange connecting the CF to the CTB is also a feedthrough, which allows the busbars, cooling lines and instrumentation lines to pass from the cryostat vacuum into the CTB vacuum.

#### 2.1.8.3 Coil Terminal Box and Structure Cooling Valve Boxes

The CTBs provide the housing for interconnection of the magnet systems with the cryoplant, the power supplies, and the data acquisition system, and they also house the local cryogenic control components. Valves in the CTBs control the mass flow rate of helium for each coil and each structural element. These valves are also used during cool-down and warm-up operations to control thermal gradients.

All CTBs contain one pair of current leads making the transition from the superconducting helium cooled busbars inside the CTB to the room temperature busbars from the power supply. The number and capacity of the current leads are shown in Table 2.1.8-2. Type F and V current leads, as shown in the Table, are optimized for constant and variable current, respectively.

**Table 2.1.8-2 Number and Capacity of Current Lead**

Coils	Number of pairs	Maximum Current (kA)	Type	Maximum Voltage (kV)
TF Coil	9	68	F	10
PF Coil	6	45	V	14
Correction Coil	9	8	V	3
CS Coil	6	45	V	10

The Structure Cooling Valve Boxes (SCVBs) contain the remotely controlled helium valves for each structural system. The structure cooling for 18 TF coils and PF coil supports includes two SCVBs. The structure cooling for the CS coil system includes one SCVB.

#### 2.1.8.4 Instrumentation

The functions of the instrumentation system are:

- to detect superconductor quench, electrical insulation faults and other abnormal conditions, and trigger protective energy discharge through the interlock system,
- to monitor coil, feeder and current lead parameters as part of normal machine operation and, if set points are exceeded, notify the operator through the alarm system,
- to measure the cooling and thermo-hydraulic parameters and calculate the required mass flow rates.

The function of the control system is to operate the CTB and SCVB coolant valves to provide the required mass flows to the coils, current leads and structures.

The magnet system contains many different sensors. Each sensor measures a specific physical parameter of the magnet system (voltage, helium mass flow, pressure, temperature, strain, displacements, etc.). For quench detection, redundant quench detection sensors (voltage and mass flow) and wiring are used inside the cryostat for reliability. To limit the possibility of short circuits and ground faults, only voltage taps (no sensors) are connected to the conductors, and each voltage tap has a current-limiting resistor in series to prevent short circuits through the instrumentation wire.

The magnet instrumentation and control systems consist of the following items.

##### i) Magnet local panels

The magnet local panels condition the analog signals from the sensors, and perform analog-digital signal conversions to interface with the computers including the magnet controller. The panels also detect quenching of the superconductors, receive signals from the power supplies and, through hard-wired interlocks, can trigger a fast protective discharge of the coil energy. The panels are placed close to the CTBs, in the galleries which are accessible for hands-on maintenance.

##### ii) The magnet controller

The magnet controller is used for the interface to the supervisory control system of CODAC. It summarises data from the local panels for central monitoring.

### 2.1.9 Magnet Safety

Magnet safety has received particular attention because of the large energy inventory and therefore the potential albeit hypothetical influence of magnet failures on other components, especially those associated with nuclear confinement. Magnet faults (whether or not they involve external components) can have a severe effect on the overall machine availability, and the repair is difficult, so there are multiple monitoring and protection systems built into the design. These include inherent features, detection/monitoring systems (that operate continuously while the coils are charged), and testing systems (that are applied periodically when plasma pulsing is interrupted or when the magnets are discharged). Particular attention is paid to reducing the probability of potential cascade sequences, where the existence of an initial fault increases the probability of others (for example, heat from a short degrades a protection barrier or increases local voltages), and common mode faults where several components (due, for example, to a common design or manufacturing error) have the same initial fault.

All initial faults have some form of protection, either active or inherent in the design, that prevents them leading to events that can cause damage to the magnets or surrounding components. Only a series of faults can lead to damage. As the final result of a safety-related event sequence, various primary 'damage mechanisms' have been identified for the magnets. It is found that all potential damage mechanisms which can affect the nuclear components (either the cryostat, the vacuum vessel or the pipework and ducting within the cryostat) are associated with molten material produced by arcing.

Arcing between conductors and structures within the cryostat is prevented by the use of a hard ground system for the structures and the cryostat walls, and by ensuring that all live conductors are within a robust grounded containment.

Contrary to general expectations, shorts that develop inside coils do not lead to significant arcing and the damage can be confined to the coil. However, external shorts on the CS and PF busbars (superconducting or normal) can potentially lead to molten material generation in the coils themselves (not significantly in the busbars) due to the coupling of extra energy into the coil, followed by a quench that cannot be discharged. Due to the thin confinement cases on these coils, a substantial fraction of this molten material could enter the main cryostat (1,000 kg would be a conservative estimate). Due to the location of the PF coils, most of it would be deposited onto the thermal shields and the vacuum vessel, although distributed over several square metres in the toroidal direction. The vacuum vessel is sufficiently robust to withstand this form of distributed heating (most arc accidents will, however, be associated with helium leakage from the affected coil into the cryostat, and with failure of the feedthroughs in the cryostat wall).

### 2.1.10 Supporting R&D and General Assessment

The model coil projects were launched to drive the development of the ITER full scale conductor, including the manufacturing of strand, cable, conduit and termination, and the conductor R&D in relation to AC losses, stability and joint performance. These projects also drive the supporting R&D programmes on coil manufacturing technologies, including the entire winding process (wind, react, and transfer), electrical insulation and quality assurance.

*Strand for the Model Coil Programme*

The total planned production of 29 t of Nb<sub>3</sub>Sn strand, from seven different suppliers throughout the four original ITER Parties, has been completed and qualified. This reliable production expanded and demonstrated the industrial manufacturing capability which will be required for the production of 480 t of high performance Nb<sub>3</sub>Sn strand for ITER.

### *CS Conductor and Coil Manufacture*

The size of the CS model coil (3.6 m in diameter and 2 m in height) is almost the same as the size of a ITER CS module (4 m in diameter and 2 m in height) and the maximum field and coil current are also the same.

The manufacture of the inner module (USA), the outer module (Japan), and the CS type insert coil (Japan) were completed during 1999. This manufacture has allowed to establish the cabling, jacketing and winding techniques with a conductor very similar in size to the full size CS conductor. The heat treatment, to react the superconducting alloy without degrading the mechanical properties of the Incoloy 908 jacket, is a critical step which has also been successfully completed. The assembly of the two coil modules and the CS type insert coil was completed before the end of 1999 (Figure 2.1.10-1). In April 2000, the maximum field of 13 T and stored energy of 640 MJ, at a maximum current of 46 kA, have been achieved in the ITER dedicated test facility at JAERI-Naka (Figure 2.1.10-2). This full charge has been followed by a comprehensive test programme including current-sharing temperature measurements, AC loss measurements, fast ramp-up and fast discharges, and current and field cycles simulating the ITER CS operation. Although the analysis of the data is not complete, it is already clear that the performance of the CS model coil is broadly according to expectations and meets the full size CS operation conditions. A 10,000 cycles fatigue test of a Nb<sub>3</sub>Sn insert coil (JAHT) has also been completed and results are under evaluation.

N 13 GR 30 00-12-07 W 0.1



**Figure 2.1.10-1 CS Model Coil and CS Insert Installed in the Vacuum Chamber at the Test Facility in JAERI Naka**

N 13 GR 31 00-12-07 W 0.1

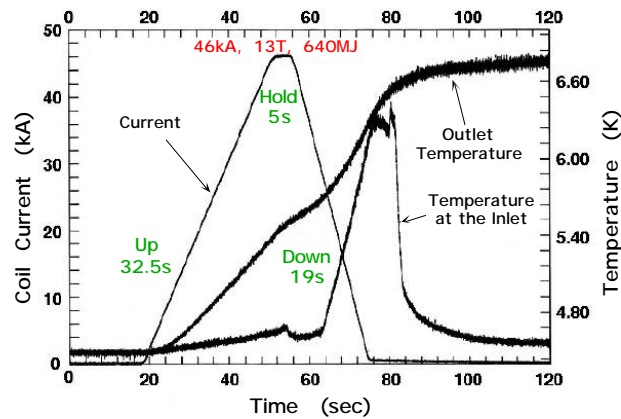


**Figure 2.1.10-2 Ramp-up to 46 kA, 13 T, Flattop of 5 s, followed by Ramp-down to Zero**

### *TF Conductor and Coil Manufacture*

The model coil uses a cable similar to the full size TF coil cable and the cross section of the TF model coil is smaller but comparable in design (use of radial plates) to that of the ITER TF coil.

The manufacture of the TF model coil was completed by the beginning of 2001. This manufacture has allowed the techniques which will be used for the manufacture of the full size coils to be established:

- forging and machining of the radial plates (Figure 2.1.10-3);
- cabling, jacketing, winding, reaction treatment, and transfer of the conductor on the radial plates;
- impregnation of the double pancakes and winding pack, insertion of the winding pack in the case, closure weld of the case and final impregnation.

All this work has been performed in the EU. The coil testing is expected to start in June - July 2001. The model coil will be tested first on its own and later in conjunction with the LCT coil in the TOSKA facility at FzK (Germany). With the LCT coil, a field of 9.7 T at 80 kA will be achieved. By comparison, the peak field and the operating current are 11.8 T and 68 kA in ITER.

N 11 GR 567 00-12-07 W 0.1



**Figure 2.1.10-3 Winding TF Model Coil Conductor into Mould**

A test up to 13 T of the TF type insert coil with a single layer of conductor will be performed in the CS model coil test facility at JAERI. The manufacture of this insert coil has been completed in the Russian Federation and the insert was delivered to the JAERI test facility in May 2001. Testing will take place during the 2<sup>nd</sup> half of 2001. A 1 km jacketing test, which exceeds the ITER requirements, has been separately demonstrated in the Russian Federation.

#### *TF Coil Cases*

For the development of the manufacture of the TF coil case, large forged (Figure 2.1.10-4) and cast pieces (about 30 t and 20 t respectively) have been produced in the EU. The use of forgings and castings is attractive since it is expected to result in significant cost reductions as compared to a manufacture based on welded plates. Investigation of the properties of the forging has revealed values exceeding the requirements of 1,000 MPa yield stress and 200 MPam<sup>1/2</sup> fracture toughness, with low fatigue crack growth rates. The casting also shows properties adequate for the low stress regions of the case (yield stress about 750 MPa). Welding trials have demonstrated successful welding of the cast to forged sections, and have established welding procedures for the case sections and the final closure weld of the half cases.

N 11 GR 568 00-12-07 W 0.1



**Figure 2.1.10-4 Forging of Inner Leg Curved Section of TF Coil Case as Hollow Tube**

*New R&D Activities*

New R&D requirements have been identified to improve the database, allow cost reductions and address technology needs specific to the ITER design. As already indicated, they cover the insulation materials and shear keys, the pre-compression rings of the TF coil structure, the radial plate manufacture, the materials and manufacturing technology database for the jacket of the CS conductor, and the CS pancake joint performance.

An R&D programme on NbTi conductors and joints for the PF coils has been launched. Results have already been obtained on investigations of strand coatings for AC loss control. Testing of conductor and joint samples are planned. The manufacture of a NbTi insert coil is an essential part of this programme. The design of this NbTi insert coil is underway and manufacture is planned to take place in 2002. The testing of the insert will take place at the JAERI test facility in 2003.

*General Assessment*

The ITER magnet design is well advanced, and design solutions have been identified. The R&D programme launched in 1993 is near its completion. This programme has confirmed the manufacturing feasibility of the conductor and the magnets. The experimental results achieved with the CS model coil and CS insert are excellent and confirm the adequacy of the conductor to meet the ITER CS operation conditions. New R&D activities have been launched to facilitate cost reductions and address certain specific technology needs.